



The effect of wall roughness on the liquid removal in micro-channels related to a proton exchange membrane fuel cell (PEMFC)

Guangli He^a, Yohtaro Yamazaki^{a,*}, Abuliti Abudula^b

^a Department of Innovative and Engineered Materials, Interdisciplinary Graduate School of Science and Engineering, Tokyo Institute of Technology, Japan

^b North Japan New Energy Research Center, Hirosaki University, Aomori, Japan

ARTICLE INFO

Article history:

Received 11 June 2009

Received in revised form

28 September 2009

Accepted 29 September 2009

Available online 7 October 2009

Keywords:

Micro-channel

Roughness

VOF

Contact angle

Simulation

PEMFC

ABSTRACT

In this paper, the effect of the wall roughness on the water behavior related to the PEMFCs gas channel is investigated by the two-phase flow simulation. And, the different wetting conditions of the wall surface are considered, i.e. hydrophilic surface and hydrophobic surface. The relative roughness height and the roughness element density as well as the roughness element type are also considered in the study. And the results show: (1) for hydrophilic surface, water behavior for smooth case is different from the roughness cases, due to the effect of roughness on the water slug morphology even for $r/H=0.2\%$ roughness. (2) $r/H=0.2\%$ is positive for water removal and will not lead to the high pressure drop for hydrophilic surface, (3) $r/H=5\%$ is advantageous for water removal for hydrophilic surface but disadvantageous for hydrophobic case, and the pressure drop greatly increases for both cases, (4) for hydrophobic surface, roughness of $r/H=1\%$ and $r/H=2\%$ slow down the water removal speed, but will not affect the amount of the removable water, (5) there is nearly no effect for $r/H=0.2\%$ for hydrophobic case, (6) for both conditions, the average pressure drop obviously increases when $r/H \geq 2\%$. (7) Increase of the roughness element can help water removal for hydrophilic case but no obvious function for hydrophobic surface. (8) The triangle roughness element is better than rectangle element with the same height.

© 2009 Elsevier B.V. All rights reserved.

1. Introduction

Proton exchange membrane fuel cells (PEMFCs) are regarded as the most promising energy conversion systems for future automobiles and stationary applications, and water management is the key issue in PEMFCs, which is a significant technical challenge. Liquid water transport in PEMFCs occurs as follows: (1) Water is produced in cathode catalyst layer, and liquid water transports within the gas diffusion layer (GDL) by capillary-driven flow. (2) Liquid water droplets appear on the GDL/gas channel interface and are removed by the gas shearing function [1–4]. (3) Liquid water travels in the gas channel with interaction with channel walls [5,6].

Due to the importance and the complexity of water transport behavior in PEMFCs, which is also difficult to observe or measure by the experiment. Many models have been developed for simulating the liquid water transport in PEMFCs. Those models are based on the different theory and assumption in flow dynamics. One of the most commonly used model is the multiphase mixture model, which consider the liquid and the gas as mixture [7–10] simply and calculation cost effectively. In the recent works, the two-fluid model has obtained more attention for its convenience of consid-

ering the liquid phase and gas phase separately, so it can describe more phenomenons in two-phase flow [11–13]. However, both the multiphase mixture model and the two-fluid model cannot involve the effect of the gas channel wall properties such as contact angle. Then, VOF (volume of fluid) model is applied into the simulation of liquid behavior in PEMFCs. The application of VOF model in PEMFCs simulation is concentrated on the two kinds of phenomena, one is the effect of gas channel contact angle on liquid removal in gas channel [14–17], the other is about the detachment behavior of a droplet on the GDL surface [18–21]. For the gas channel walls, the contact angle determines the channel wall is hydrophilic or hydrophobic, and then determines the shape and form of liquid water slug when it contacts with the gas channel walls. However, there is also another important factor for the gas channels, i.e. wall roughness, which may affect the flow resistance. And, there is no relevant work to consider the effect of the gas channel roughness on the liquid water removal now. But actually, at the micro-scale level, it is impossible to obtain a completely smooth wall surface. According to the traditional knowledge for macro-systems, when the relative roughness is less than 5%, its effect on the friction factor is negligible. But for micro-scale channels, previously reported experimental and computational results have drawn a conclusion that surface roughness has a significant influence on flow and heat transfer [22–25]. For example, the experiment by Kandlikar et al. [22] indicated that for a 0.62 mm tube with relative

* Corresponding author. Tel.: +81 45 924 5411.

E-mail address: yamazaki.y.af@m.titech.ac.jp (Y. Yamazaki).

roughness of 0.355%, the effect of roughness on the friction factor and heat transfer was significant. Mala and Li [26] observed that for rough channels with diameters ranging from 50 to 254 μm (relative roughness height 0.7–3.5%), the pressure gradient was higher than that predicted by the classical theory and the friction factor increased when the Re number was increased. In addition, an early transition from laminar to turbulent flow occurred at the Reynolds number less than 2300. They concluded that these phenomena can be well explained due to the surface roughness effects. While E. Ciulli [27] developed an equivalent smooth model for the micro-system for the seal application.

However, nearly all of the references are concentrated on the single phase behavior, but for the two-phase flow in micro-scale channels, there is no relevant research. In this paper, we try to consider the effect of the gas channel wall roughness on the water behavior, and make insight into the water flow in the channel, then may provide some guidelines for the operation of the PEMFCs and the manufacture of the gas channels.

2. Simulation methods and procedures

2.1. VOF model for simulation

In this study, a VOF (volume of fluid) model is used to simulate the liquid water behavior in the gas channel. The VOF formulation relies on the fact that two-phase fluids are not interpenetrating and a phase indicator function of the *k*th phase $\alpha_k(t, r)$ based on the volume fraction, which marks the *k*th phase fluid position when the fluid moves through the fixed mesh, is tracked. $\alpha_k(t, r)$ is the function of time, *t*, and space, *r*, defined as the ratio of the volume of the *k*th phase in the computational cell to the volume of the computational cell. The function $\alpha_k(t, r)$ is evaluated on the discrete grid as a volume average, for computational cell *i*, as follows:

$$\alpha_{k,i} = \frac{1}{V_i} \int \alpha_k(t, r) dV_i \quad (1)$$

where if $\alpha_k = 1$, it means the computational cell full of the *k*th phase, $\alpha_k = 0$ means the computational cell void of the *k*th phase, $0 < \alpha_k < 1$ means the computational cell partially full of the *k*th phase and containing the gas–liquid interface. The tracking of the phase indicator function α_k and the identification of the location and shape of the interface between the gas–liquid phases are accomplished by solving the volume fraction continuity equation for each phase, expressed as:

$$\frac{\partial \alpha_k}{\partial t} + u_j \frac{\partial \alpha_k}{\partial x_j} = 0 \quad (2)$$

And the sum of the all phases' volume fraction equals unity:

$$\sum \alpha_k = 1 \quad (3)$$

Eqs. (2) and (3) are the governing equation of volume fraction, also, in VOF model, a set of the equations including the continuity equation and the Navier–Stokes momentum equation are used to describe all fluids in the motion of the unsteady, viscous, immiscible two-phase flow system, which can be expressed as:

$$\frac{\partial \rho}{\partial t} + \nabla \cdot (\rho u) = 0 \quad (4)$$

And momentum equation:

$$\frac{\partial(\rho u)}{\partial t} + \nabla \cdot (\rho u u) = -\nabla p + \nabla \cdot [\mu(\nabla u + \nabla u^T)] + \rho g + F \quad (5)$$

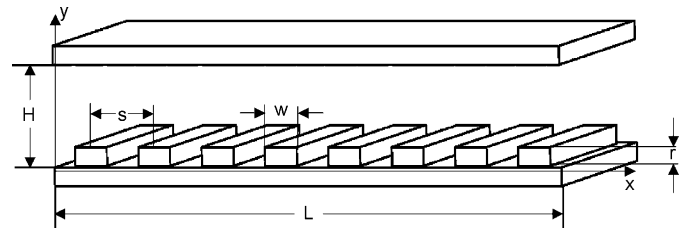


Fig. 1. Schematic view of the roughness elements.

where *F* is the force source term due to surface tension and wall adhesion:

$$F = 2\sigma k_k \frac{\rho \nabla \alpha_k}{\sum \rho_k}, \quad F_{vol} = \sum_{pairs\ ij, i < j} \sigma_{ij} \frac{\alpha_i \rho_i \kappa_j \nabla \alpha_j + \alpha_j \rho_j \kappa_i \nabla \alpha_i}{(1/2)(\rho_i + \rho_j)} \quad (6)$$

where k_k is computed from local gradients in the surface normal at the interface:

$$k_k = \nabla \cdot \left(\frac{n}{|n|} \right), \quad n = \nabla \alpha_k \quad (7)$$

The properties (ρ, μ) used in the above equations (Eqs. (4) and (5)) are the volume averaged density and dynamic viscosity, which are expressed as follows:

$$\rho = \sum \alpha_k \rho_k \quad (8)$$

$$\mu = \sum \alpha_k \mu_k \quad (9)$$

Here, for the case of liquid water moves in the gas channel in this paper, there are two phases, i.e. gas phase and liquid phase, the pressure difference in the two phases on either side of the interface can be expressed by Laplace's formula:

$$P_L - P_G = \sigma k_k \quad (10)$$

2.2. Geometry model and the initial conditions for the unsteady simulation

The roughness elements on the gas channel wall are regarded as the rectangle ribs as shown in Fig. 1. And *H*, *L*, *s*, *w*, and *r*, are the height of the channel, length of the rough area, distance between the two adjacent roughness element center, width of the roughness element and height of the roughness element, respectively. So, the ratio between *s* and *H* represents the density of the roughness element, high *s* means low numbers of roughness elements, and the relative roughness height is defined by the ratio between *r* and *H*.

Water flow in the gas channel is a dynamic process, so the simulation should be performed in the unsteady state, and the

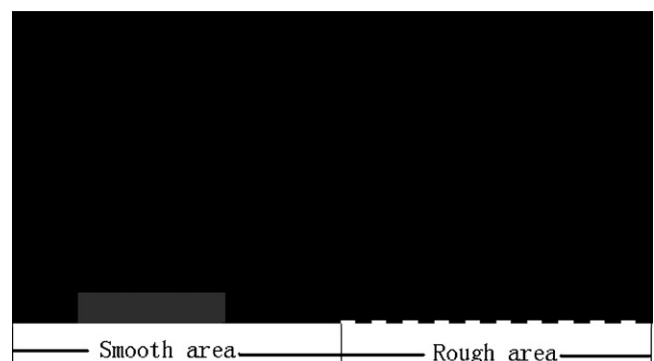


Fig. 2. Initial condition for the unsteady simulation.

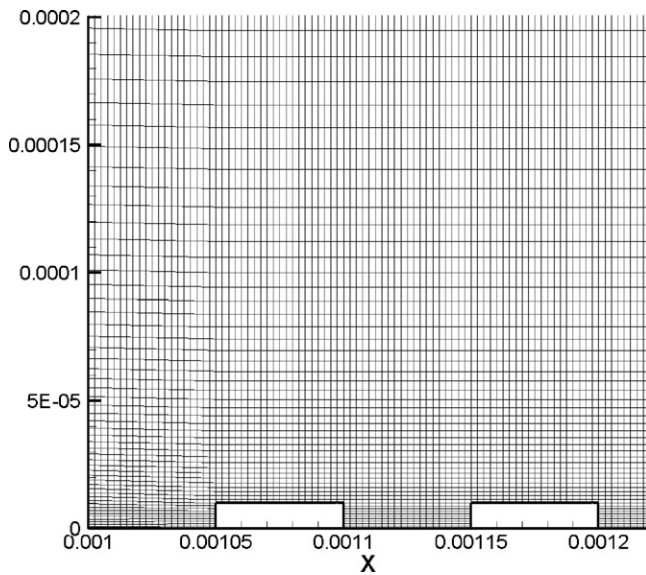


Fig. 3. Local grid for the roughness element.

initial condition should be specified. Fig. 2 shows the initial condition of the simulation. The liquid water is initially a water film ($0.5 \text{ mm} \times 0.1 \text{ mm}$) on the smooth surface, and flow to the rough area driven by the gas until the removable water fully flows out. The initial inlet velocity is 8 m s^{-1} , which is suitable for the practical small fuel cells. For all the cases, the contact angle is 90° in the smooth area, and the shape of the water film is consistent with the contact angle, so the same liquid volume is obtained for all the cases, which is the base for the comparison of results for different rough cases.

2.3. Discretization and solution method

The fluids are assumed to be incompressible and isothermal and to have constant fluid properties. The finite volume method is used to discretize the transport equation. There are totally about 44,000 non-uniform grids in the domain, as shown in Fig. 3. Many methods are used to improve the accuracy and convergence of the VOF solution. The quick differencing scheme is used for solving the momentum equation to minimize numerical diffusion and the first-order explicit time marching scheme is used for solving the unsteady formulation. The interface between gas and liquid are reconstructed using piecewise linear interface calculation (PLIC) proposed by Young. To improve a rapid convergence rate without any significant loss of accuracy, the pressure-implicit with splitting of operators (PISO) pressure-velocity coupling scheme, which is based on the higher degree of the approximate relation between the corrections for pressure and velocity, is used for the pressure-velocity scheme. The time step size is $2e-7 \text{ s}$, maximal iterations per time step is 200, and the converge criterion for all the variables are $1e-6$. And the simulation is performed in Fluent[®] software of Ansys company.

Table 1
Different cases for simulation.

Case	L (mm)	H (mm)	r (% H)	s (% H)	Contact angle	w (s%)
1	1.05	1	0	10	$30^\circ, 60^\circ, 120^\circ, 150^\circ$	50
2	1.05	1	0.2	10	$30^\circ, 60^\circ, 120^\circ, 150^\circ$	50
3	1.05	1	1.0	10	$30^\circ, 60^\circ, 120^\circ, 150^\circ$	50
4	1.05	1	2.0	5, 10, 20	$30^\circ, 60^\circ, 120^\circ, 150^\circ$	50
5	1.05	1	5.0	10	$30^\circ, 60^\circ, 120^\circ, 150^\circ$	50
6 (Tri)	1.05	1	2.0	10	$30^\circ, 150^\circ$	50

2.4. Validity of grid independence and time step independence

For the unsteady simulation, grid size and time step size can both affect the results. So the independence of these two variables are checked. Calculation for 1.5 times grid numbers and 2 times grid numbers as well as different time step size ($1e-7 \text{ s}$ and $3e-7 \text{ s}$) are all done, and no obvious difference is observed. So, we think it has the grid independence and time step independence.

3. Results and discussions

The simulation for different relative roughness and contact angle of the channel wall, as well as the different roughness elements are simulated (Table 1). And the conditions for the simulation are listed in the following:

3.1. The effect of roughness on water removal for different surface condition

In the application of PEMFCs, the water contact angle of the gas channels is also an important factor, and the contact angle can affect the flow behavior of the liquid water, so in the investigation of the effect of the water roughness on the water removal, the contact angle is also in consideration, and the research is performed with different contact angle condition, i.e. hydrophilic condition (30° and 60°) and hydrophobic condition (120° and 150°). And the results are discussed for the different wetting condition separately.

In the evaluation of the water removal, two variables are essential, i.e. the flow rate and the water accumulation ratio. The fast flow rate for water removal and the low water accumulation ratio are pursued for the design of the gas channel. The water accumulation ratio is defined as follows:

$$r = \frac{V_r}{V_{init}}$$

which, the V_r is the water remained in the gas channel and V_{init} is the initial water volume in the gas channel or the water produced by the electrochemical reactions, so the water accumulation ratio represents the water removal efficiency. In this paper, these parameters are mainly investigated for different roughness cases and hydrophilic/(hydrophobic) cases.

3.1.1. The effect of relative roughness on the water removal for hydrophilic surface

Figs. 4 and 5 show the water mass flow rate at the outlet for the different roughness cases, in which the relative roughness height ranges from 0% to 5% with the contact angle of the surface being 30° and 60° , respectively. It can be seen that the time for the water beginning to flow out are different for the different relative roughness, and the time sequence for different roughness is $0\% < 0.2\% < 1\% < 2\% < 5\%$, that means the roughness really have effect on the water behavior, and the existence of the roughness height slow down the water flow speed, even though the roughness height is as small as 0.2%. It can be seen also that the motion of the water in the gas channel for the different roughness height is different. Firstly, for all the cases, there is a maximum peak of the flow rate,

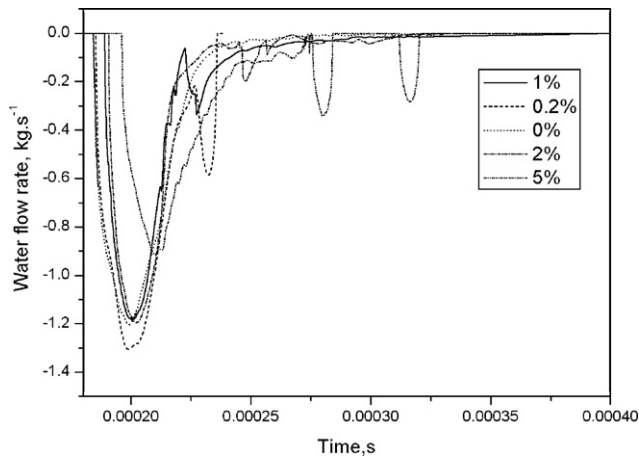


Fig. 4. Water flow rate at outlet for different relative roughness height of 30°.

which means the water flows out in the form of nearly droplet, so most of the water is removed in very short time, that is the common point. But secondly, for the no roughness case, the flow rate curve versus time is like a parabola, while the curves for other roughness are composed of more than one parabola especially for the 5% case, there are nearly four parabolas. That means the flow pattern for the water removal is different. It is more likely that water flows out in the continuous way for the no roughness case, but the liquid slug changes to more than one part for the roughness cases. To demonstrate this, the water distribution for the different cases at the same time are shown in Figs. 6–8, for 0 and 0.2%, 2% cases at $t = 2e-4s$, respectively. It is obvious that the liquid water flow morphology is different, and the liquid water in the rough gas channel is more likely be separated into a few water slugs. So, in this way, we can see that the roughness has effect on the water flow by affecting the liquid water slug morphology, while the roughness relative height reaches 5%, the water behavior for removal is totally different from the low roughness relative height occasions.

The effect of the roughness relative height on the water flow rate at outlet is mainly investigated above. And, the water accumulation ratio in the gas channel is also very important for evaluating the performance of water removal. Figs. 9 and 10 show the water accumulation ratio with the flow time for the contact angle of 30° and 60° separately. It can be seen that the final water accumulation ratio are different for the different cases, which means that the roughness not only has effect on the water flow rate at outlet but also affect the water accumulation in the gas channel. And

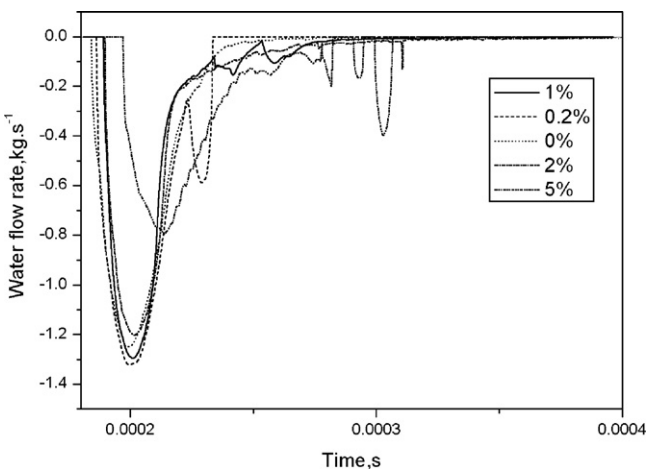


Fig. 5. Water flow rate at outlet for different relative roughness height of 60°.

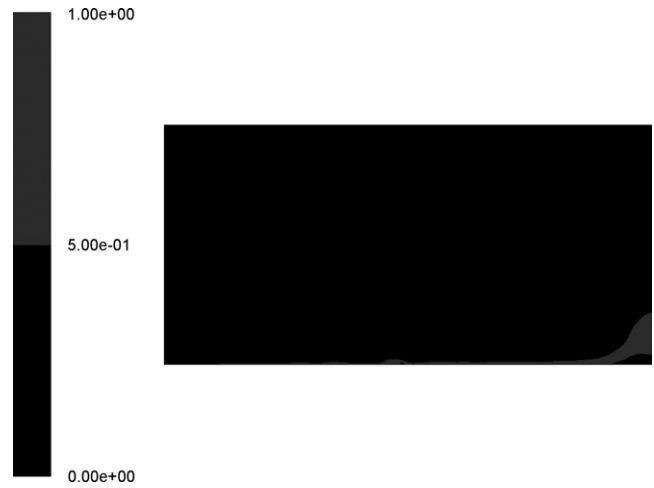


Fig. 6. Water distribution for smooth case at $t = 2e-4s$.

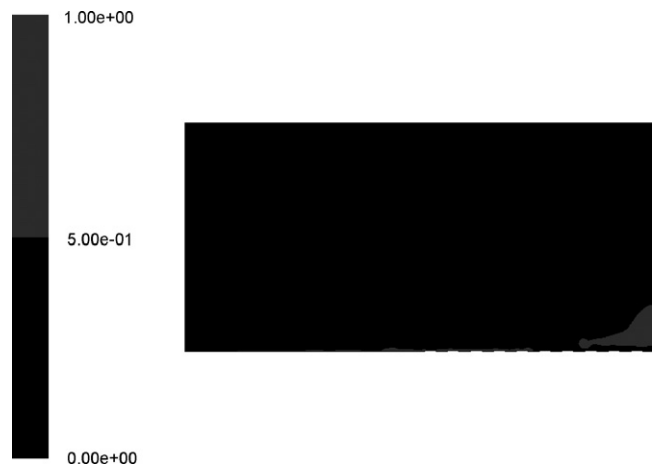


Fig. 7. Water distribution for $r/H = 0.2\%$ case at $t = 2e-4s$.

Figs. 9 and 10 clearly show that the final water accumulation ratio for the 0.2% and 5% cases are nearly the same, which are lower than that of smooth case, and water accumulation ratio for the 1% and 2% cases are also nearly the same, which are high than that of smooth case. Due to the conclusion that the roughness has effect on the water flow out pattern, i.e., the water removes in the continuous way for the smooth case but flows out in the separated way for the

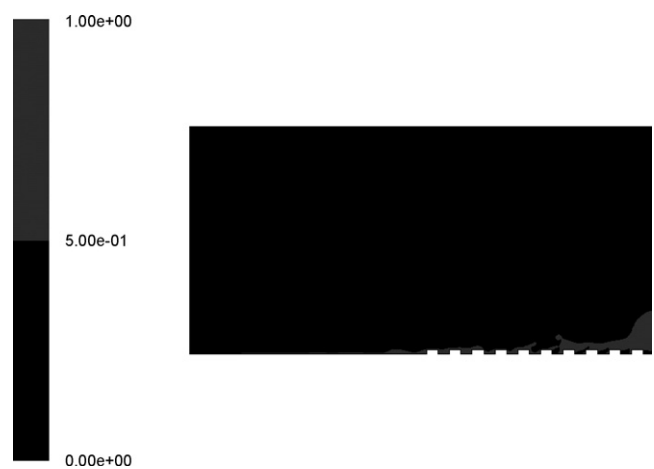


Fig. 8. Water distribution for $r/H = 2\%$ case at $t = 2e-4s$.

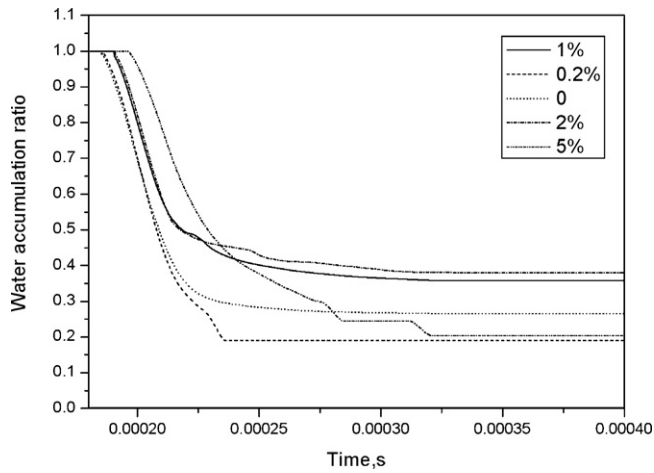


Fig. 9. Water accumulation ratio for different relative roughness height of 30°.

rough cases. So, the fact that final water accumulation ratio for 0.2% and 5% cases are low than smooth case means the suitable roughness can also improve the water removal for its effect on the water flow out pattern. Also, according to the results in Figs. 9 and 10, we can see that the 0.2% and 5% case have positive effect on the liquid water removal. But for the 1% and 2% cases, the effect is negative in the view of water accumulation ratio. Which may be caused by the fact that there are two functions for the effect of roughness on the water removal, the first function is hindering the removal of the fluid, and the second function is affecting the water slug morphology due to its unsmooth surface. And these two functions have the opposite effect on the water removal. The final result is determined by the dominant one.

3.1.2. The effect of relative roughness on the water removal for hydrophobic surface

Figs. 11 and 12 show the water flow rate at outlet for the different roughness height for the contact angle of 120° and 150° (hydrophobic case), respectively. As shown in Figs. 11 and 12, the water flow rate curve with time for the hydrophobic smooth case is different from the hydrophilic smooth case, which includes two parabolas means the water is not removed in the continuous way, and this is due to the effect of the hydrophobic surface tension, which makes the liquid water is in the form of droplet, so the liquid water flow out by the different droplet. It also can be seen that the flow rate for the 5% case is different from the other cases, which is caused by the effect of the roughness height, i.e. the roughness

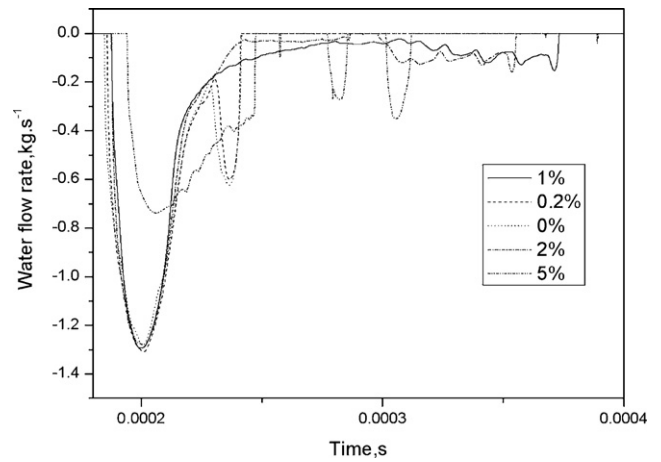


Fig. 11. Water flow rate at outlet for different relative roughness height of 120°.

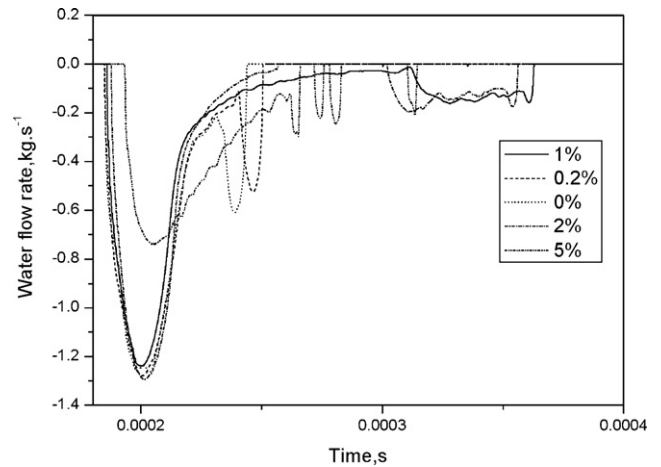


Fig. 12. Water flow rate at outlet for different relative roughness height of 150°.

height greatly hinders the flow of the liquid and affects the water droplet morphology.

Figs. 13 and 14 show the water accumulation ratio for different relative roughness height for the contact angle of 120° and 150°, respectively. It can be seen that the final accumulation ratio for the smooth case, 0.2%, 1%, and 2% are nearly the same, which is smaller than that of 5% case. That means the effect of the roughness height on the water droplet morphology is limited for hydropho-

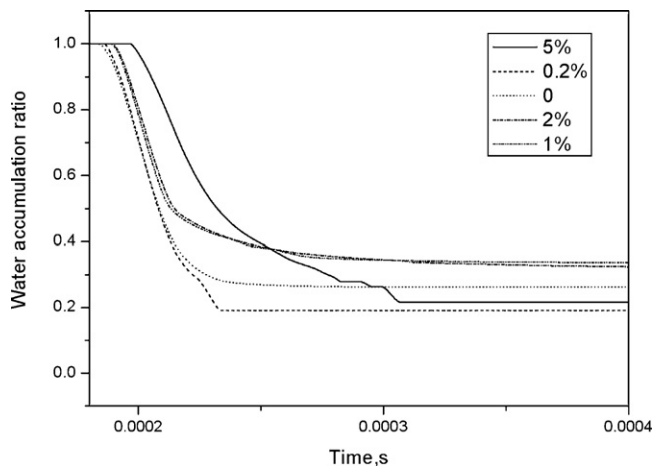


Fig. 10. Water accumulation ratio for different relative roughness height of 60°.

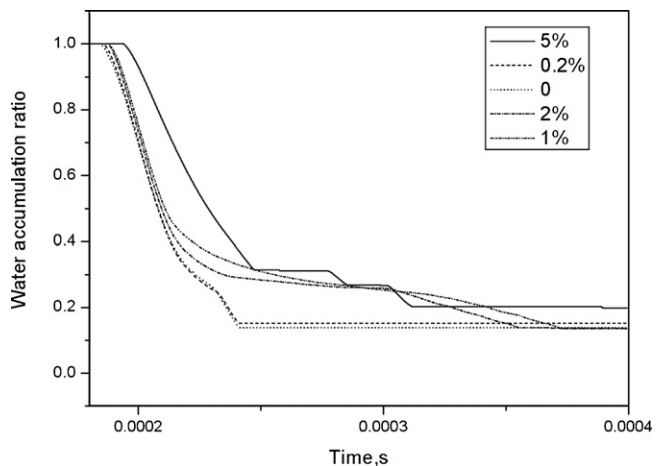


Fig. 13. Water accumulation ratio for different relative roughness height of 120°.

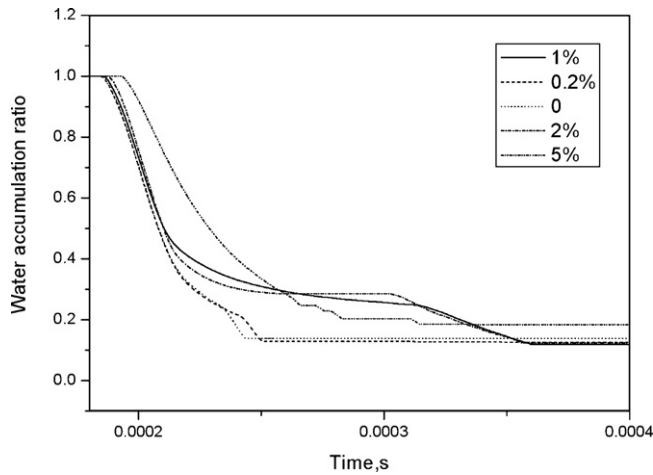


Fig. 14. Water accumulation ratio for different relative roughness height of 150°.

bic case for the liquid water is already in the form of droplet due to the surface tension. Although the same final accumulation ratio, the time cost for the water removal (from beginning to the constant accumulation ratio) are different for different roughness height, and the time for the 0, and 0.2% case are nearly same, which means the effect of 0.2% roughness height can be neglected, but for relative roughness height larger than 1%, the effect is very notable, and should be considered. So, the small roughness (1%, 2%) can slow down the water removal speed, but will not affect the amount of the removable water, but when the roughness reaches 5%, the accumulation ratio and removal speed are both be affected negatively.

3.2. The effect of roughness on the pressure drop

Pressure drop during the flow is also an important parameter for evaluate the performance of the gas channel, which indicates the flow resistance, and low flow resistance is the aim of the flow in the gas channel. However, in the present study, the simulation is performed in the unsteady state for investigating the liquid water behavior, so the time average pressure drop from the beginning time to the time when the liquid flows out the gas channel (when the water flow rate is zero, and the accumulation ratio retains constant) is chosen as the representative of the flow resistance. Fig. 15

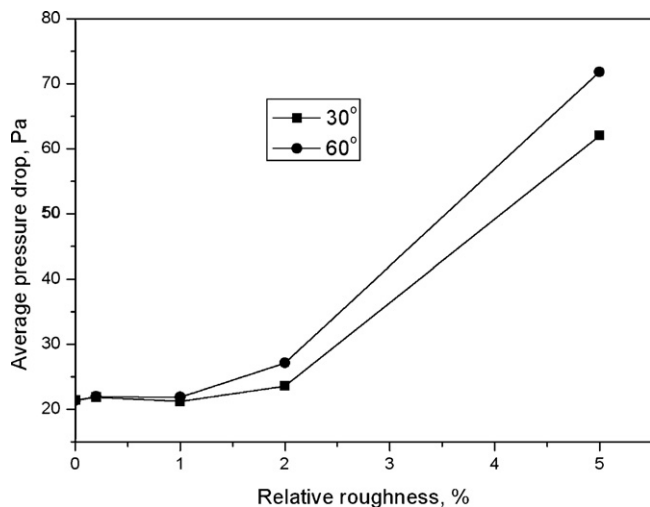


Fig. 15. Average pressure drop for the hydrophilic cases for different roughness height.

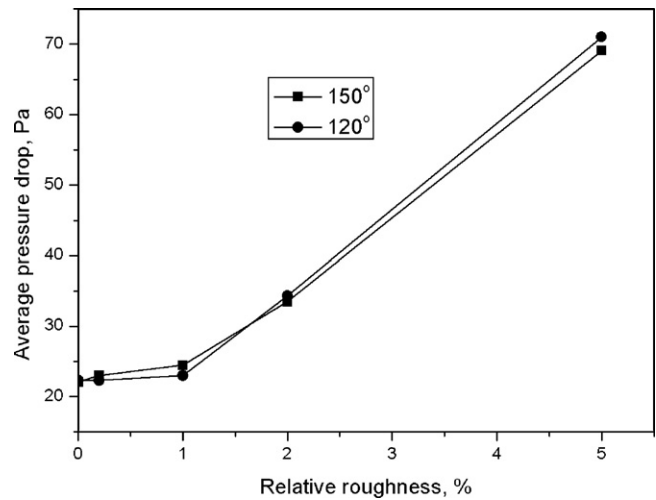


Fig. 16. Average pressure drop for the hydrophobic cases for different roughness height.

shows the average pressure drop for different cases for the 30° and 60°. It can be seen that the average pressure drop increases with increase of the relative roughness height, especially for the relative roughness height is larger than 1%. When the relative roughness reaches 5%, the pressure drop is largely increased. The pressure drop also increases with the contact angle increases.

Fig. 16 shows the average pressure drop for the hydrophobic case. Also, it is obvious that the pressure drop increases with the increase of the roughness height when the relative roughness height is greater than 1%. When the relative roughness reaches 5%, the pressure drop is largely increased. But only small changes can be observed between the different contact angles. So, in the view of the pressure drop, roughness greater than 1% can increase the flow resistance.

3.3. The effect of the roughness density (numbers of the roughness element) on the water removal

In evaluation of the roughness, there is another very important parameter except for the roughness height, that is roughness density (which is the numbers of the roughness elements in the same area), and high roughness density means more roughness elements, while low roughness density means less roughness elements. And the numbers of the roughness element is measured by the ratio between s and H (channel height).

In this paper, the effect of the numbers of roughness on the water flow is also investigated. Figs. 17 and 18 show the water accumulation ratio with the flow time for the 2% case for three different numbers of roughness elements, i.e. 5%, 10% (base case) and 20% for the hydrophilic case (30°) and hydrophobic case (150°). It can be seen that the water accumulation ratio decreases with the increase of the roughness element for the hydrophilic case, but only slight changes for the hydrophobic case. To see insight of this phenomenon, the water distribution for $s=5H$ and $s=20H$ for the 30° case are shown in Figs. 19 and 20, respectively at $t=3.2e-4s$. It is obvious that it is difficult to wet the roughness element with increase of the roughness element numbers, i.e. with decrease of the roughness element size for the hydrophilic case, the difficulty for wetting increases, so it hinders the liquid water to flood every element fully, so the water accumulation ratio decreases. As for the hydrophobic case, the contact angle is 150° already, and the water cannot wet the surface even if without roughness element, so the effect of the numbers of roughness element is very limited.

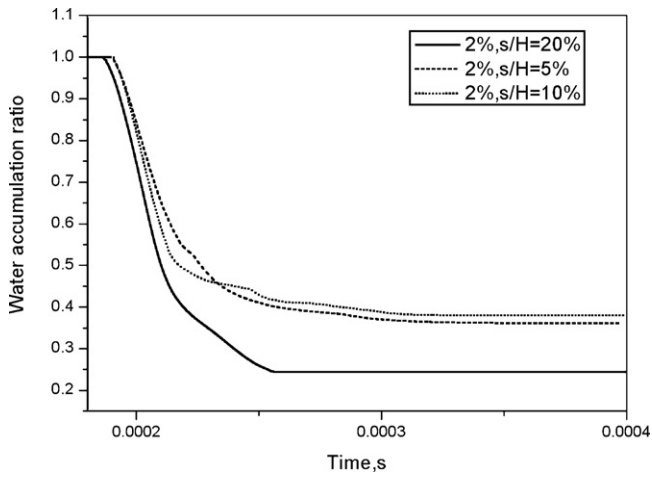


Fig. 17. Water accumulation ratio for different roughness density of 30° and $r/H=2\%$ case.

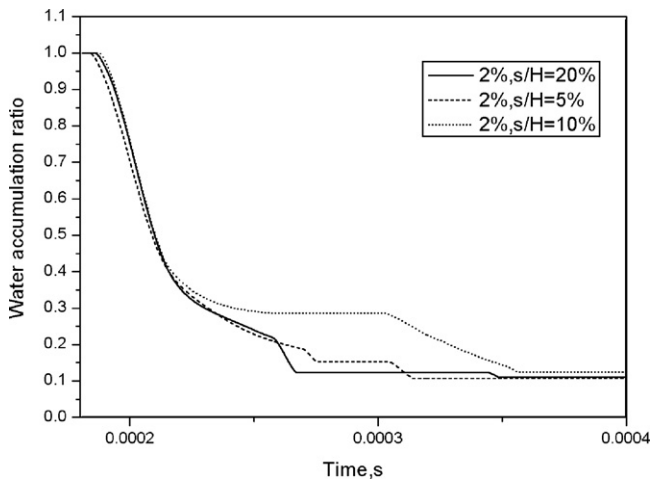


Fig. 18. Water accumulation ratio for different roughness density of 150° and $r/H=2\%$ case.

3.4. The effect of the roughness element type

In the actual manufacture of the surface, the roughness element type is not certain, it maybe rectangle type, triangle type or other types. To investigate the difference of the water removal

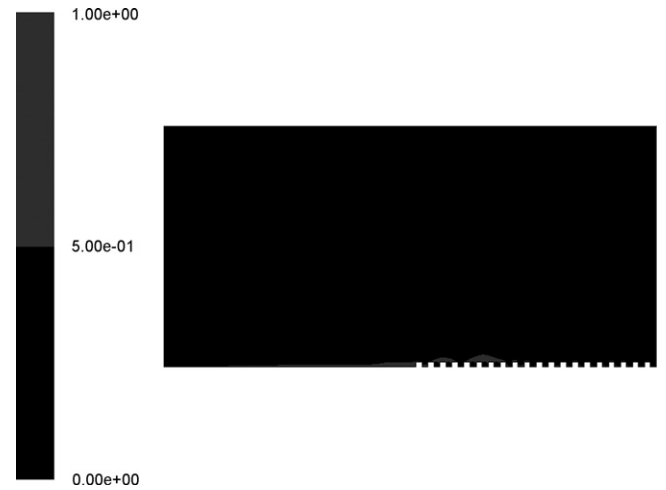


Fig. 20. Water distribution for $s/H=20\%$, and $r/H=2\%$ case of 150° at $t=3.2e-4s$.

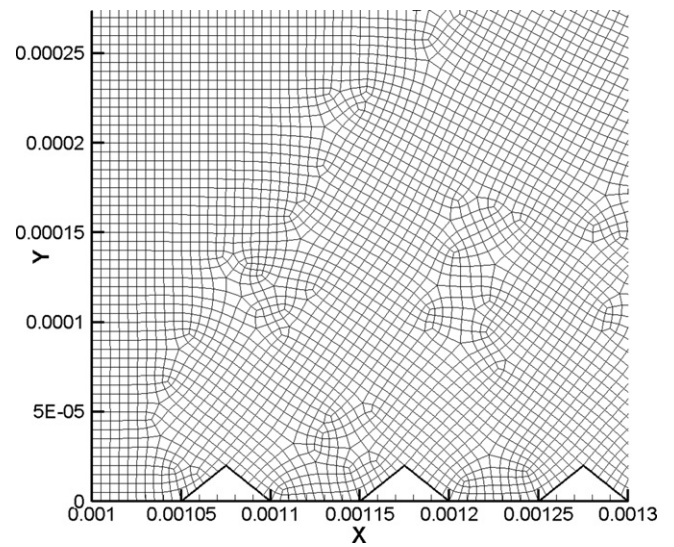


Fig. 21. Grid for triangle roughness element.

for different roughness element type, the water behavior for the gas channel wall with triangle roughness element is also simulated. Fig. 21 shows the grid for the triangle roughness element. Figs. 22 and 23 show the water accumulation ratio and average

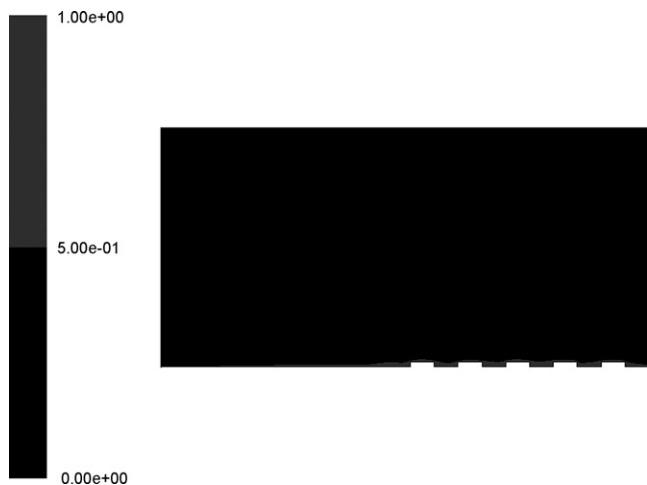


Fig. 19. Water distribution for $s/H=20\%$, and $r/H=2\%$ case of 30° at $t=3.2e-4s$.

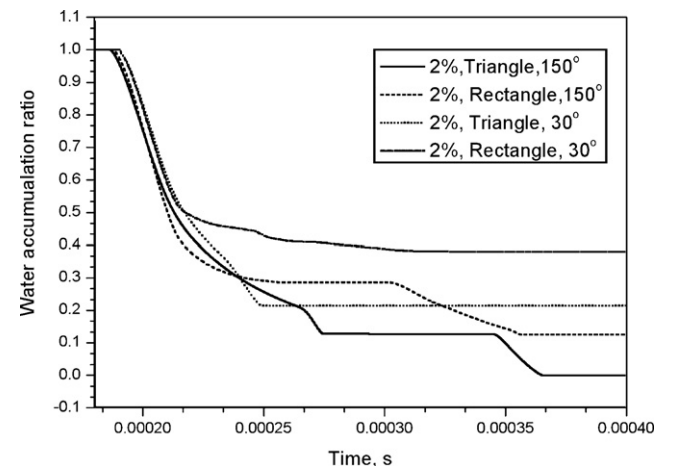


Fig. 22. Accumulation ratio for triangle roughness element.

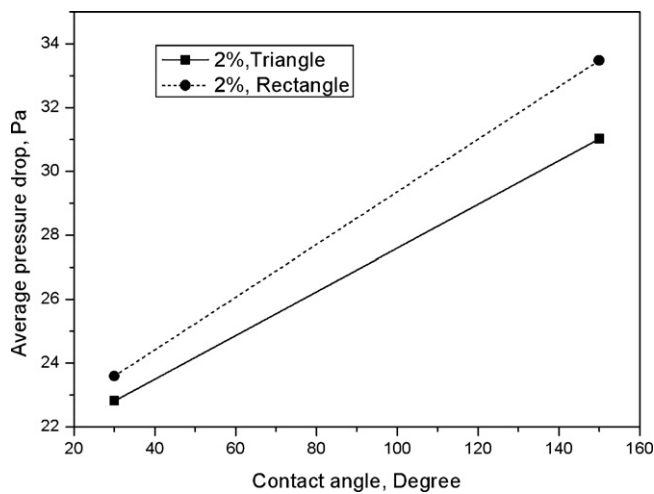


Fig. 23. Average pressure drop for different roughness element type.

pressure drop for $r/H=2\%$ of hydrophilic case (30°) and hydrophobic case (150°), respectively. It can be seen obviously that the final accumulation ratio of triangle roughness element type is less than that of rectangle type case both for hydrophilic case and hydrophobic case in Fig. 22. That means the triangle roughness element is better than rectangle roughness element with the same height for less water accumulation. Besides, Fig. 23 shows that the average pressure drop for the triangle roughness element is also less than that of rectangle roughness element. So, we can see that the triangle roughness element is better than rectangle roughness element with the same height both for water accumulation and for pressure drop.

4. Conclusions

In this paper, the simulation with VOF model is performed to investigate the effect of the roughness on the water behavior related to the PEMFCs gas channel. And, the different wetting conditions of the wall surface are considered, i.e. hydrophilic surface and hydrophobic surface. The relative roughness height with 0, 0.2%, 1%, 2% and 5%, are investigated for both wetting conditions. The contact angles for the hydrophilic surface are 30° and 60° , while 120° and 150° for hydrophobic surface. The effect of the roughness element density and the roughness element type are also considered in the study. The water flow rate at outlet, the water accumulation ratio, and the average pressure drop are mainly investigated for the different conditions. And the results show:

- (1) For hydrophilic surface, water behavior for smooth case is different from the roughness cases, due to the effect of roughness on the water slug morphology even for $r/H=0.2\%$ roughness.
- (2) For hydrophilic surface, $r/H=0.2\%$ is positive for water removal and will not lead to the high pressure drop.

- (3) $r/H=5\%$ is advantageous for water removal for hydrophilic surface, but disadvantageous for hydrophobic case, and the pressure drop greatly increases for both cases.
- (4) For hydrophobic surface, roughness of 1% and 2% slow down the water removal speed, but will not affect the amount of the removable water.
- (5) There is nearly no effect for $r/H=0.2\%$ for hydrophobic case.
- (6) For both conditions, the average pressure drop obviously increases when $r/H \geq 2\%$.
- (7) Increase of the roughness element can help water removal for hydrophilic case but no obvious function for hydrophobic surface.
- (8) The triangle roughness element is better than rectangle element with the same height.

References

- [1] K. Tüber, D. Póczy, Christopher Hebling, Journal of Power Sources 124 (2003) 403–414.
- [2] A. Hakenjos, H. Muentert, U. Wittstadt, C. Hebling, Journal of Power Sources 131 (2004) 213–216.
- [3] X.G. Yang, F.Y. Zhang, A.L. Lubawy, C.Y. Wang, Electrochemical and Solid-State Letters 7 (2004) A408–A411.
- [4] K.S. Puneet, P. Halleck, C.-Y. Wang, Electrochemical and Solid-State Letters 9 (2006) A344–A348.
- [5] A. Bazylak*, J. Heinrich, N. Djilali, D. Sinton, Journal of Power Sources 185 (2) (2008) 1147–1153.
- [6] F.Y. Zhang, X.G. Yang*, C.Y. Wang, Journal of the Electrochemical Society 153 (2) (2006) A225–A232.
- [7] H. Sun, H. Liu, L.-J. Guo, Journal of Power Sources 143 (2005) 125–135.
- [8] Z.H. Wang, C.Y. Wang, K.S. Chen, Journal of Power Sources 94 (2001) 40–50.
- [9] U. Pasaogullari, C.-Y. Wang, K.S. Chen, Journal of the Electrochemical Society 152 (2005) A1574–A1582.
- [10] H. Meng, C.-Y. Wang, Journal of the Electrochemical Society 152 (2005) A1733–A1741.
- [11] G. He, P. Ming, Z. Zhao, A. Abudula, Y. Xiao, Journal of Power Sources 163 (2007) 864–873.
- [12] K. Jain, J. Vernon Cole, S. Kumar, A. Gidwani, N. Vaidy, ECS Transactions 16 (2) (2008) 45–56.
- [13] T. Berning, ECS Transactions 16 (2) (2008) 23–34.
- [14] P. Quan, M.-C. Lai, Journal of Power Sources 164 (2007) 222–237.
- [15] Y.H. Cai, J. Hu, H.P. Ma, B.L. Yi, H.M. Zhang, Journal of Power Sources 161 (2006) 843–848.
- [16] Z. Zhan, J. Xiao, M. Pan, R. Yuan, Journal of Power Sources 160 (2006) 1–9.
- [17] P. Quan, B. Zhou, A. Sobiesiak, Z. Liu, Journal of Power Sources 152 (2005) 131–145.
- [18] C. Fang, C. Hidrovo, F.-m. Wang, J. Eaton, K. Goodson, International Journal of Multiphase Flow 34 (2008) 690–705.
- [19] X. Zhu, P.C. Sui, N. Djilali, Journal of Power Sources 172 (2007) 287–295.
- [20] X. Zhu, P.C. Sui, N. Djilali, Journal of Power Sources 181 (2008) 101–115.
- [21] A. Theodorakakos, T. Ous, M. Gavaises, J.M. Nouri, N. Nikolopoulos, H. Yanagihara, Journal of Colloid and Interface Science 300 (2006) 673–687.
- [22] S.G. Kandlikar, S. Joshi, S. Tian, Proceedings of NHTC.01 35th National Heat Transfer Conference, Anaheim, CA, June, 2001, pp. 1–10.
- [23] Y. Hu, C. Werner, D. Li, ASME Journal of Fluids Engineering 125 (2003) 871–879.
- [24] Y. Ji, K. Yuan, J.N. Chung, International Journal of Heat and Mass Transfer 49 (2006) 1329–1339.
- [25] G. Croce, P.D. Agaro, Superlattices and Microstructure 35 (2004) 601–616.
- [26] G.M. Mala, D. Li, International Journal of Heat Mass Transfer 20 (1999) 142–148.
- [27] J.R. Valdés, M.J. Miana, J.L. Pelegay, J.L. Núñez, T. Pütz, International Journal of Heat and Mass Transfer 50 (2007) 1865–1878.